Application of Advanced Wall-Functions to Forced and Mixed Convection Flows

Dr Hector Iacovides
Department of Mechanical Aerospace and Manufacturing Engineering
UMIST

CONTENTS

1. The problem of the modelling near-wall turbulent flows.

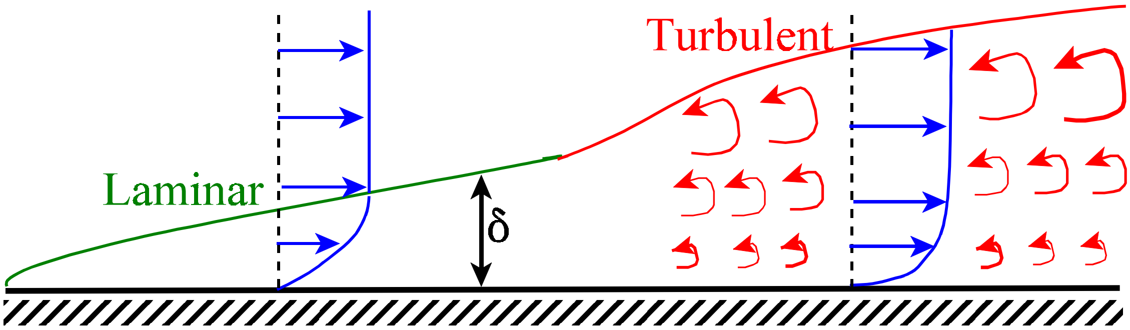

- Most flow problems in engineering applications involve **wall-bounded turbulent flows**.

- At the solid fluid interface, the no slip condition ensures that the **turbulent fluctuations vanish**.

- There is thus a very thin, but important **sub-layer** next to the wall, where transport of heat and momentum is predominately due to **molecular diffusion**.

- **Question:** How to account for this viscosity-dominated sub-layer in the numerical simulation of turbulent flows ?

Alternatives:

1. Use Low-Reynolds-number Models.

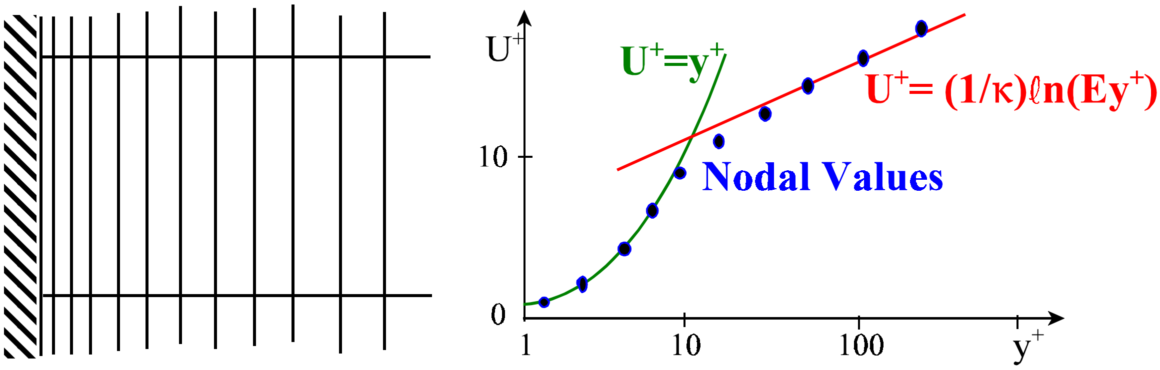

- Transport models that can be integrated across the viscous sub-layer.
- Involve no assumptions about the near-wall variation of velocity and temperature.
- Require very fine near-wall resolution.

2. Use Wall-Function Strategy.

- Computationally Efficient.

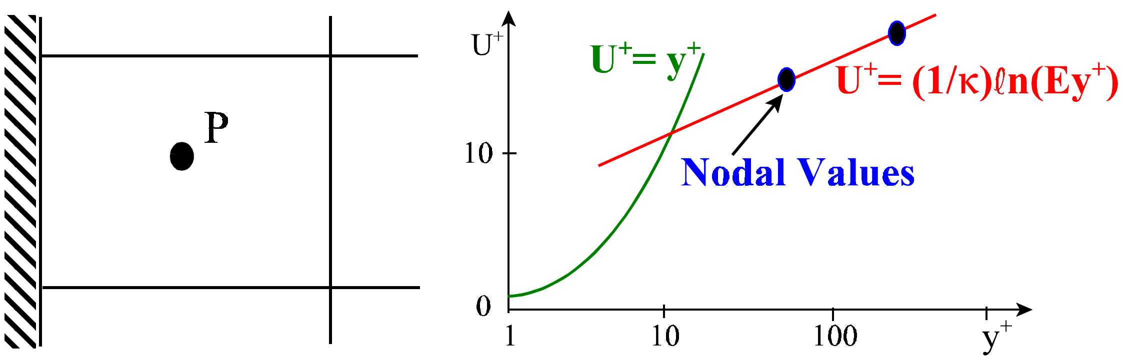

- Involve assumptions about the near-wall variation of the mean flow and of the turbulent flow parameters.

2. The Wall-Function strategy.

Overview of Wall-Function Strategy

Use of Large Near-Wall Control Volumes

Introduction of Assumptions about the Near-Wall Flow Variation

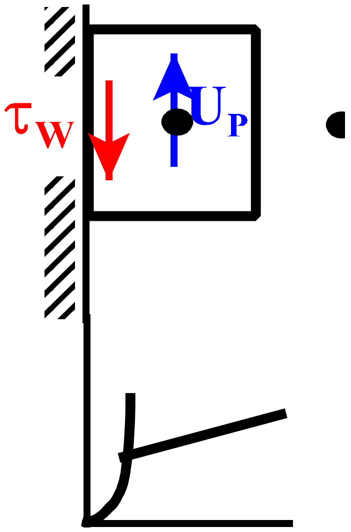

Calculation of Wall Shear Stress and Average Generation and Dissipation Rates of Turbulent Kinetic Energy for Near-Wall Contol Volumes.

Modification of Discretize Transport Equations for Wall-Parallel Momentum and Turbulent Kinetic Energy over Near-Wall Control-Volumes.

Numerical Solution of Resulting

Discretized Equations

- This framework is common to the conventional wall functions and also to the recently developed more advanced alternatives.

- The main **numerical advantage** arises from the use of **large near-wall cells**.

- **Differences** in wall functions arise from

  - The **assumptions made** about the near wall behaviour

  - The way the wall shear stress, wall temperature and cell-averaged turbulence parameters are calculated.

- The assumptions made also determine the range of flows over which the an approach can be effective.

3. Conventional Wall Functions and their limitations

■ Overview of Conventional Wall Functions

1. The **wall-parallel velocity** across most of the near-wall cell is assumed to obey the **inner law of the wall (κ=0.41)**

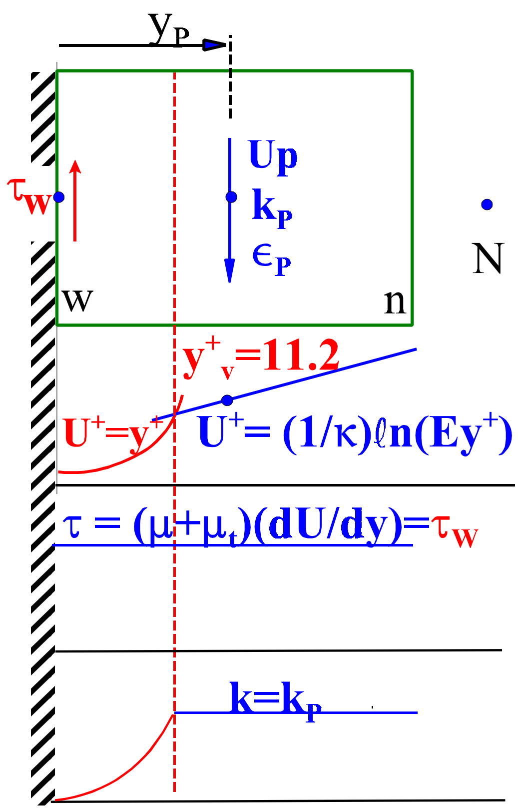

2. The **total shear stress** remains **constant** across the near-wall cell and equal to the wall shear stress.

3. The **turbulent kinetic energy** is **constant** over the inner region (=k_P) and falls quadratically to zero, in the viscous sub-layer.

4. The **dissipation rate** at the inner region is assumed to vary according to $\epsilon = k_P^{1.5}/c_\ell y$ (c_ℓ=2.55) and to remain constant across the viscous sub-layer.

▪ Limitations of Conventional Wall Functions

- Flows subjected to strong Pressure Gradients

- Strongly Heated Internal Flows

- Boundary Layer Flows with Suction Across A Porous Wall

- Mixed and Natural Convection Flows

- Separated and Impinging Flows

- Three-dimensional Boundary Layers

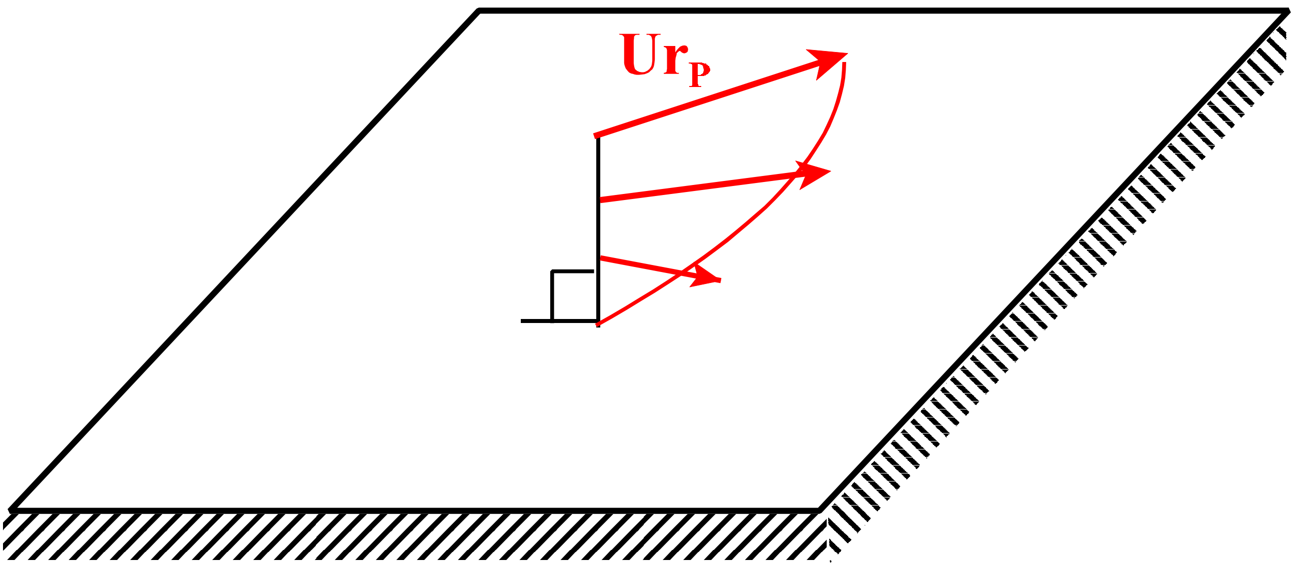

4. The UMIST approach to the development of Wall-Functions

■ **Earlier attempts to refine conventional wall functions**

- Chieng and Launder (1980)/Johnson-Launder(1982)
- Amano (1984)
- Ciofalo and Collins (1989)

● All above attempts still made use of the log-law.

■ **Current UMIST attempts**

Aim

To preserve the overall framework of the wall-function strategy, but to remove some of the more limiting assumptions made, such as the log-law and the constant total shear stress.

Approach

- The log-law is no longer used.

- The velocity and temperature variations across the near-wall cells are determined through the solution of simplified, locally one-dimensional transport equations for the wall-parallel momentum and for enthalpy.

$$\frac{d}{dy}\left[(\mu+\mu_t)\frac{dU}{dy}\right] = -\frac{d}{dx}(\rho UU) - \frac{dP}{dx} \qquad (I)$$

$$\frac{d}{dy}\left[\left(\frac{\mu}{Pr}+\frac{\mu_t}{\sigma_T}\right)\frac{dT}{dy}\right] = -\frac{d}{dx}(\rho UT) \qquad (II)$$

Where x and y the wall-parallel and wall-normal directions respectively

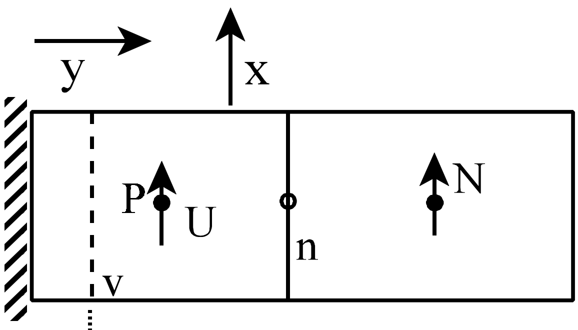

Boundary conditions:

At $y = 0$

$U=0$ And $T=T_W$

At $y = y_n$ $U_n=(U_P+U_N)/2$ $T_n=(Y_P+T_N)/2$

From the resulting velocity and temperature distributions across the near-wall cells:

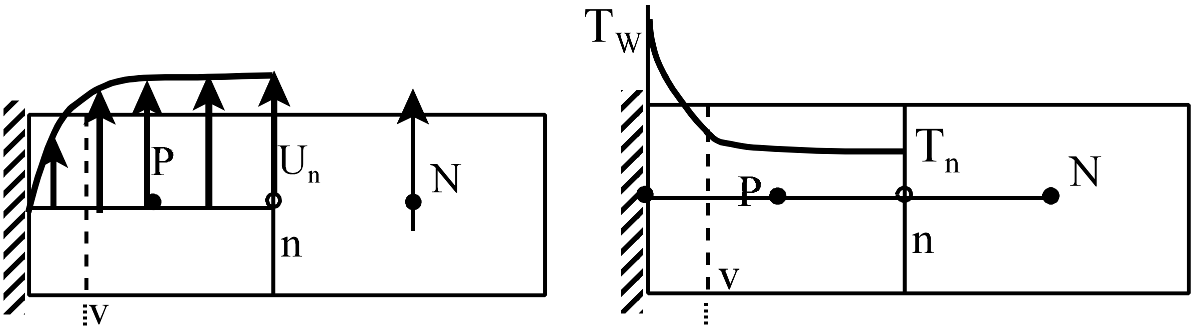

- The wall shear stress, τ_W, can be calculated

- Either the wall temperature, T_W, or the wall heat flux, q_W, can be calculated

- The cell-average P_k can be calculated

- The above parameters can be used to modify the discretized transport equations for wall-parallel momentum, enthalpy and turbulent kinetic energy over the near-wall cells.

- In three-dimensional flows, momentum transport equations in two directions can be independently solved.

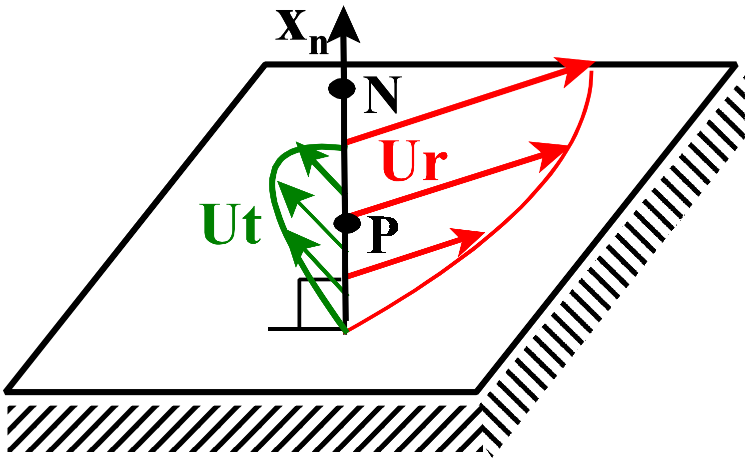

<u>Boundary Conditions</u>

At $x_n = 0$

$U_n = 0$ and $U_t = 0$

At $x_n = x_n^n$ $U_n = 0.5*(U_n^P + U_n^N)$ And $U_t = 0$

- **Alternative Strategies**

Two different strategies have been developed at UMIST for the solution of equations (I) and (II) that:

- Share the same overall approach outlined so far.
- Differ in the assumptions used and the methods employed.
- Both come under the acronym **UMIST**, denoting *Unified Modelling through Integrated Sub-layer Transport.*

The two alternatives are now separately presented.

5. The Analytical Wall-Function, UMIST-A

• Mean Flow Analysis

As the name implies, **equations (I) and (II) are solved analytically** across the near-wall cell.

This is accomplished through the use of a **prescribed variation for the turbulent viscosity**, μ_t.

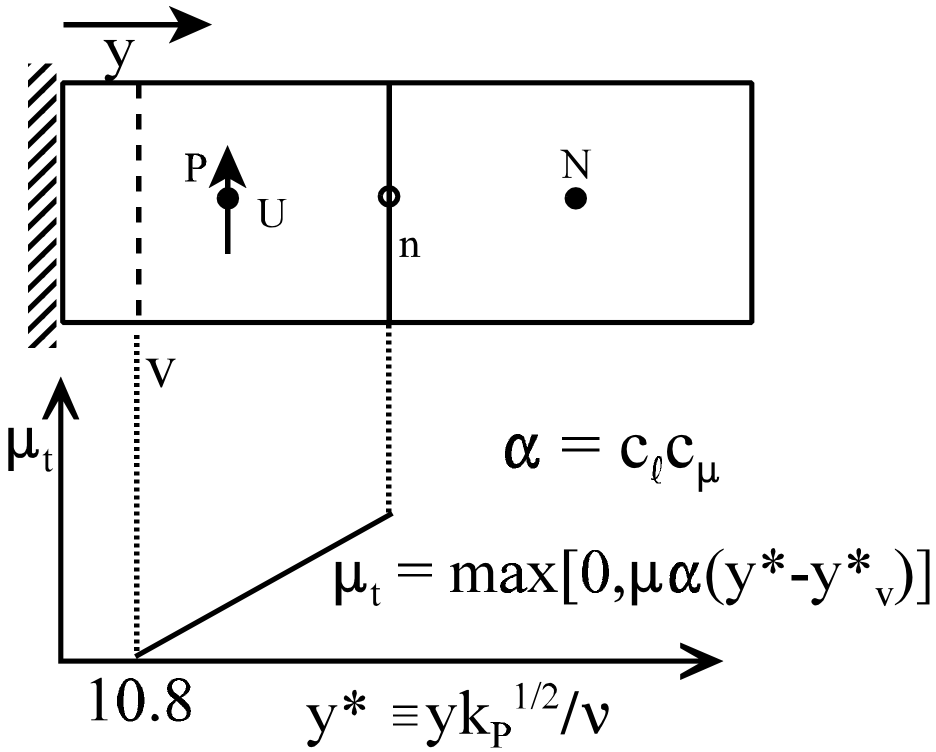

A consequence of this variation in μ_t, is that two forms of equations (I) and (II) are solved.

For $y^* < y^*_v$

$$\mu \frac{d}{dy}\left[\frac{dU}{dy}\right] = \left[\frac{d}{dx}(\rho UU) + \frac{dP}{dx}\right]_P$$

$$\frac{\mu}{Pr}\frac{d}{dy}\left[\frac{dT}{dy}\right] = \left[\frac{d}{dx}(\rho UT)\right]_P$$

For $y^*_v > y^* < y^*_n$

$$\mu \frac{d}{dy}\left[\left(1 + \alpha(y^* - y^*_v)\right)\frac{dU}{dy}\right] = \left[\frac{d}{dx}(\rho UU) + \frac{dP}{dx}\right]_P$$

$$\frac{\mu}{Pr}\frac{d}{dy}\left[\left(1 + \frac{\alpha Pr}{\sigma_T}(y^* - y^*_v)\right)\frac{dT}{dy}\right] = \left[\frac{d}{dx}(\rho UT)\right]_P$$

The right hand sides of the equations are treated as constants and are calculated from the nodal values.

At the **interface** between the two regions, y^*_v, it is required that **the variables** (U and T) and their **first derivatives** (dU/dy and dT/dy) are **continuous**.

The empirical constant y^*_v is determined as **10.8**

The **analytical integration** of the above equations results in algebraic equations that provide a **continuous variation of U and T**.

- **Wall Shear Stress and Wall Heat Flux**

Differentiation of the analytical expressions at **y=0**, will then result in:

$\tau_w = -\mu dU/dy_{y=0}$ and $q_W = -(c_P\mu/Pr)dT/dy_{y=0}$

- **Average Generation Rate, P_k**

Thus : $P_k = \alpha\mu\,(y^* - y^*_v)\,[dU/dy]^2$

$$\textit{Integrating:}\quad \overline{P_k} = \frac{\alpha\mu}{y_n}\int_{y=y_v}^{y=y_n}(y^* - y^*_v)\left(\frac{dU}{dy}\right)^2 dy$$

• Average Dissipation Rate

As in the conventional wall-functions

For $y < y_d$: $\epsilon = 2\,\nu\, k_P / y_d^{\,2}$
For $y > y_d$: $\epsilon = k_P^{3/2} / c_\ell\, y$

Unlike the conventional wall functions, case (a):

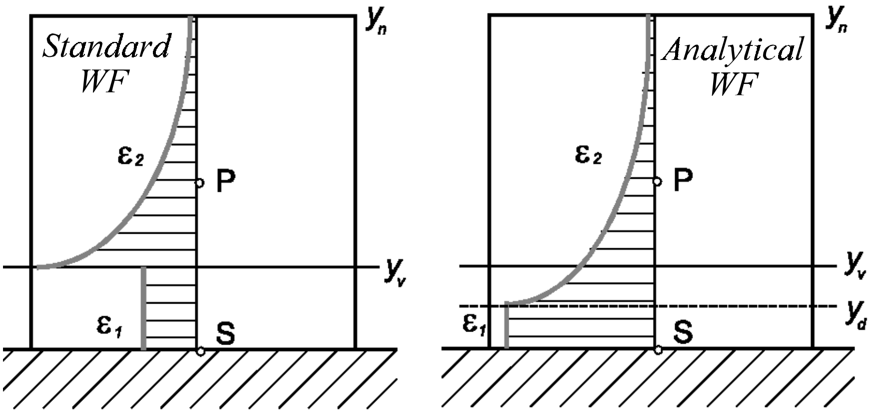

$$y^*_d \neq y^*_v \ (=20)$$

For continuity of ϵ: $2\,\nu\, k_P / y_d^{\,2} = k_P^{3/2} / c_\ell\, y_d$

$\Rightarrow$ $y_d^* = 5.1$ *Thus* $$\bar{\epsilon} = \frac{k_P^{3/2}}{y_n}\left[\frac{2}{y^*_d} + \frac{1}{c_\ell}\ell n\left(\frac{y_n}{y_d}\right)\right]$$

- **Further Extensions**

The assumptions involved are less restrictive than those in the conventional wall functions.

It is thus possible to introduce further refinements

- Introduction of **Laminarization Effects**, based on the parameter $\lambda \equiv \tau_W/\tau_v$

- **Temperature Variation** of viscosity and thermal conductivity across the viscosity-affected sub-layer.

- Inclusion of **Buoyancy Force** in the integration of the equation of the wall-parallel momentum (I) and in the disctretized momentum equation over the near-wall cells.

- **High Prandlt number correction** of the enthalpy equation (II).

- Extension to flows over **rough surfaces**, by making the sub-layer thickness, y_v^*, a function of h^*, where h is the average height of the roughness elements.

● Applications of the Analytical Wall Function

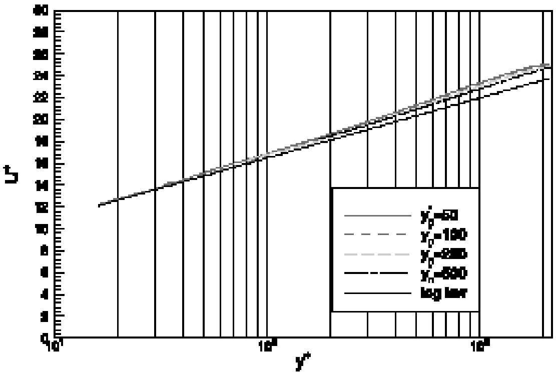

Fig. 8. Semi-logarithmic velocity profiles for $Re = 100,000$ for isothermal fully developed pipe flow.

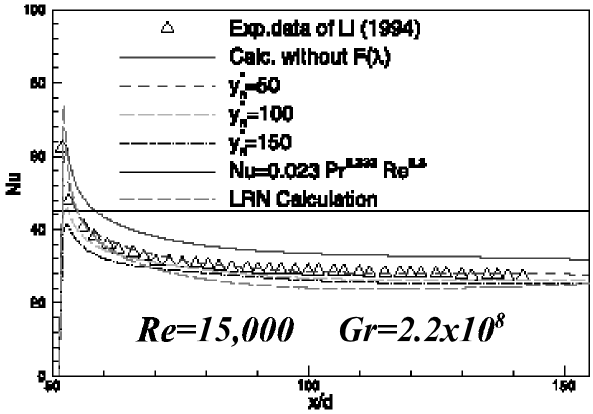

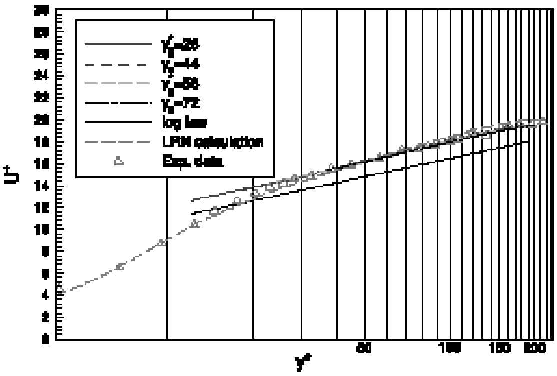

Fig. 9. Semi-logarithmical velocity profiles for $Re = 6753$ for isothermal fully developed pipe flow.

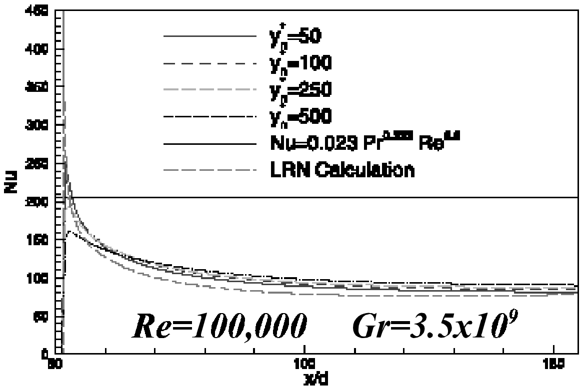

Fully Developed Pipe Flows

Developing Mixed-Convection, Upward Pipe Flows

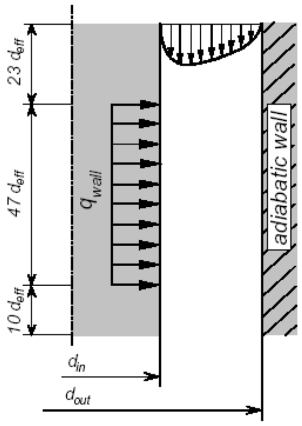

Annular Buoyancy-Opposed Flows

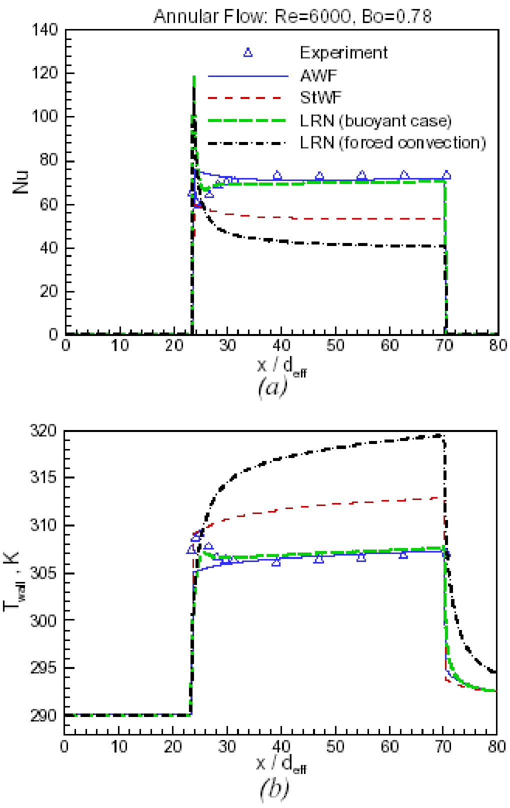

Figure 6. Predicted (a) Nusselt number and (b) wall temperature for buoyancy-opposed water flow in annulus at Bo=0.78.

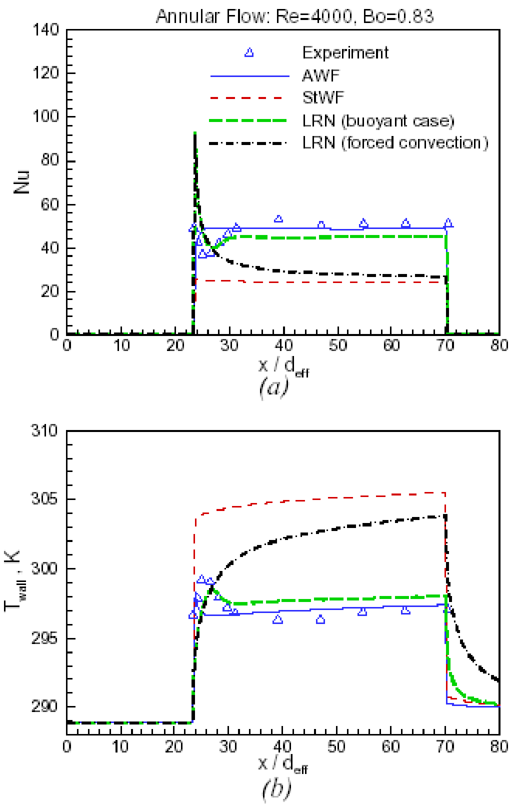

Figure 7. Predicted (a) Nusselt number and (b) wall temperature for buoyancy-opposed water flow in annulus at Bo=0.83 and Re=4000.

Flows over Rough Surfaces

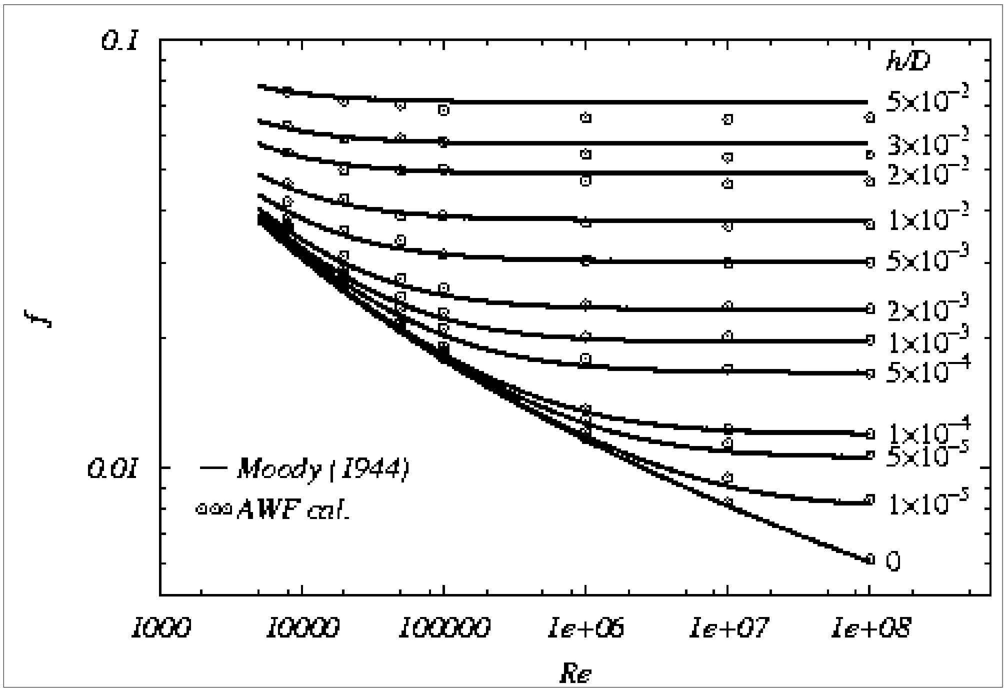

Moody Chart

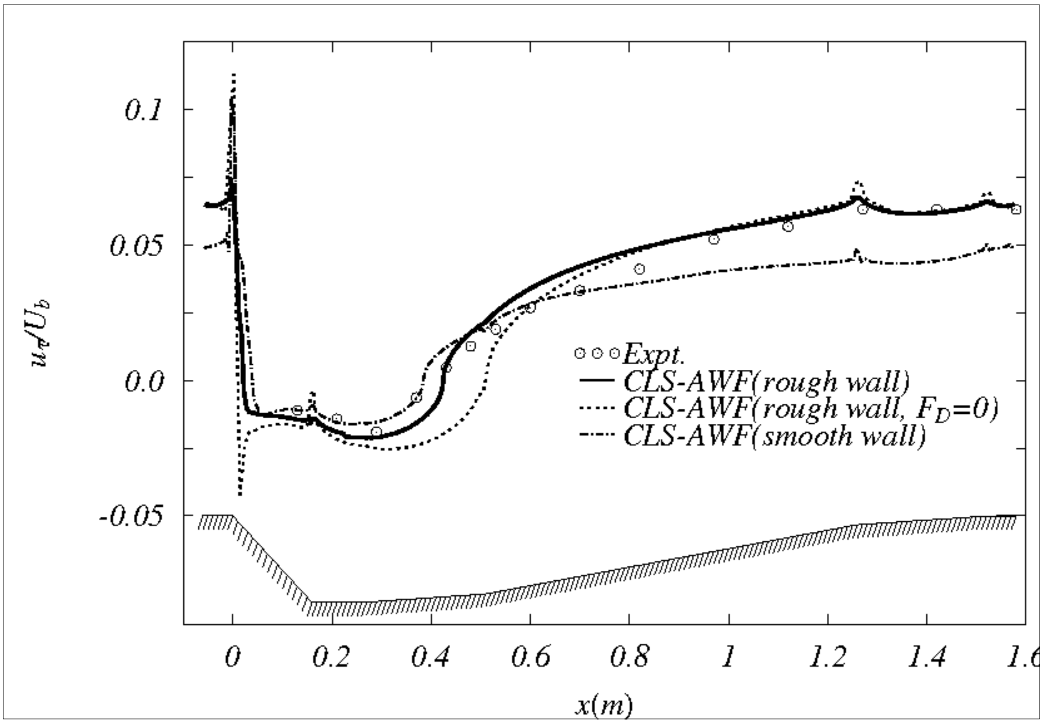

Flow over a sand-dune

Other Applications of the Analytical Wall Function

- Isothermal and non-isothermal opposed wall jets.
- Free convection boundary layer.
- Diffuser Flows
- Ribbed pipe and channel flows.
- 3-D U-Bend Flows.

6. The Numerical Wall-Function, UMIST-N

▪ Approach

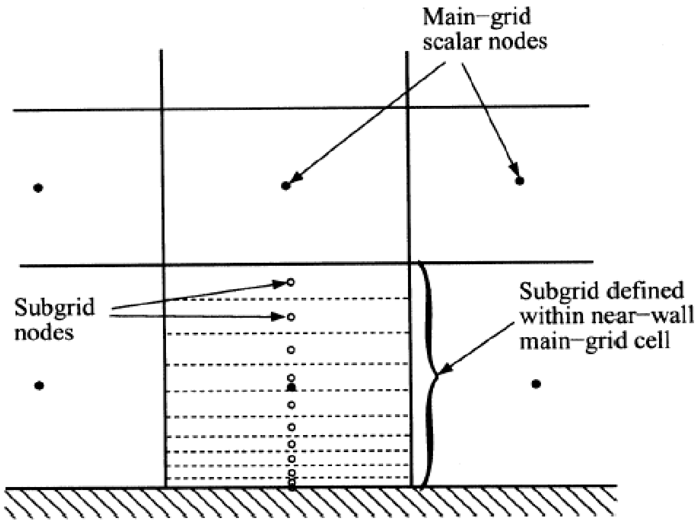

The **transport equations** for the wall-parallel momentum and enthalpy are **numerically solved** across the near-wall cells.

- Each near-wall cell is divided into **sub-volumes**.

$$\frac{d}{dy}\left[\left(\mu+\mu_t\right)\frac{dU}{dy}\right] - \frac{d}{dy}\left(\rho VU\right) = \left[\frac{d}{dx}\left(\rho UU\right) + \frac{dP}{dx}\right]_P$$

$$\frac{d}{dy}\left[\left(\frac{\mu}{Pr}+\frac{\mu_t}{\sigma_t}\right)\frac{dT}{dy}\right] - \frac{d}{dy}\left(\rho VT\right) = \left[\frac{d}{dx}\left(\rho UT\right)\right]_P$$

- **Left hand side** terms are discretized using **sub-grid nodal values**.

- **Right hand side** terms are discretized using **main grid nodal values** and are constant across each cell.

- The **wall normal velocity** at the sub-grid nodes is obtained from local sub-cell **continuity** and scaled to match the boundary nodal value.

- The **turbulent viscosity** at the sub-grid nodes is determined by numerically solving equations of a low-Reynolds-number model, over the sub-grid.

- If the Launder-Sharma is used, for example:

$$\frac{\partial}{\partial y}(\rho V k) + \left[\frac{\partial}{\partial x}(\rho U k)\right]_P = \frac{\partial}{\partial y}\left[(\mu + \mu_t)\frac{\partial k}{\partial y}\right] + P_k - \rho\epsilon - 2\rho\nu\left(\frac{\partial\sqrt{k}}{\partial y}\right)^2$$

$$\frac{\partial}{\partial y}(\rho V \epsilon) + \left[\frac{\partial}{\partial x}(\rho U \epsilon)\right]_P = \frac{\partial}{\partial y}\left[(\mu + \mu_t)\frac{\partial \epsilon}{\partial y}\right]$$

$$+ c_{\epsilon 1}\frac{\epsilon}{k}P_k - \rho c_{\epsilon 2} f_2 \frac{\epsilon^2}{k} + 2\rho\nu\nu_t\left[\frac{\partial^2 U}{\partial y^2}\right]^2 + YC$$

Terms with subscript P evaluated using main grid nodal values.

$$\mu_t = \rho\, c_\mu\, f_\mu\, k^2 / \epsilon \qquad P_k = \mu_t (dU/dy)^2$$

$$f_2 = 1 - 0.3 \exp(-R_t^2) \qquad f_\mu = \exp[-3.4 / (1 + 0.02 R_t)^2]$$

$$R_t = k^2/(\nu\epsilon)$$

▪ Implementation

- The sub-grid nodal values of the flow variables are stored for all near-wall cells.

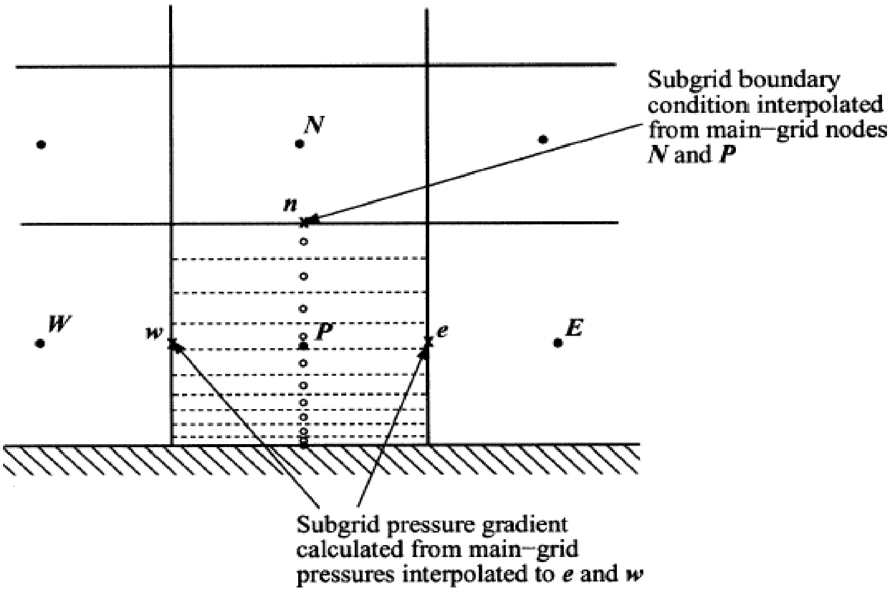

- The discretization of the wall-parallel convection ρU(dΦ/dx) is thus based on sub-grid nodal values.

- The discretization of the simplified transport equations within each near-wall cell, results in a tri-diagonal system.

$$\rho V \frac{\partial \Phi}{\partial y} - \frac{\partial}{\partial y}\left(\Gamma \frac{\partial \Phi}{\partial y} \right) = S'_{\Phi} \equiv S_{\Phi} - \rho U \frac{\partial \Phi}{\partial x}$$

$$\rightarrow \quad A_P \Phi_P = A_N \Phi_N + N\Phi_N + S'_{\Phi}$$

- The discretized sub-grid equations are solved using a **tri-diagonal matrix solver (TDMA).**

- Only one sweep of the sub-grid TDMA is performed within each iteration.
- The k and ϵ equations are under-relaxed.

- The sub-grid nodal values are used to produce:

- **Wall Shear Stress τ_W**, used to modify the discretized wall-parallel momentum equation at the near-wall cells
- Either the **wall temperature, T_W** or the **wall heat flux, q_W**, that modify the enthalpy equation at the near-wall cells.
- The **cell-averaged P_k** and ϵ that modify the k transport equation at the near-wall cells.
- The **cell-averaged**

$$c_{\epsilon 1}\frac{\epsilon}{k}P_k - \rho c_{\epsilon 2} f_2 \frac{\epsilon^2}{k} + 2\rho \nu \nu_t \left[\frac{\partial^2 U}{\partial y^2}\right]^2 + YC$$

that modify the disretized ϵ equation at the near-wall cells.

This wall-function strategy can be used with other low-Re models, such as non-linear k-ϵ models.

● Applications of the Numerical Wall Function

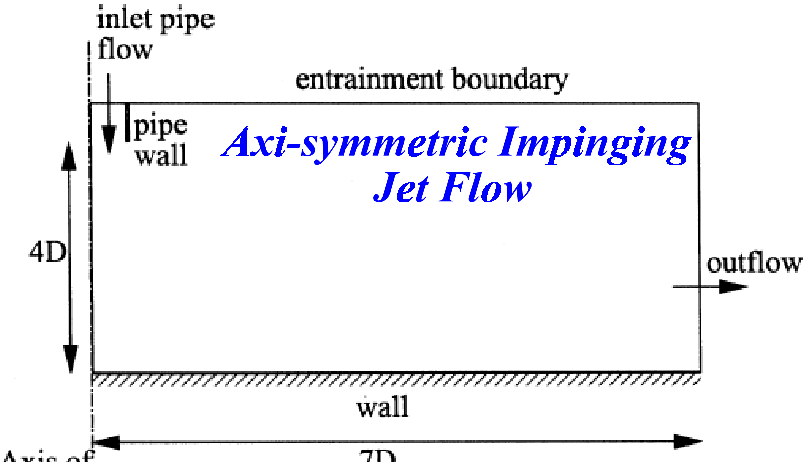

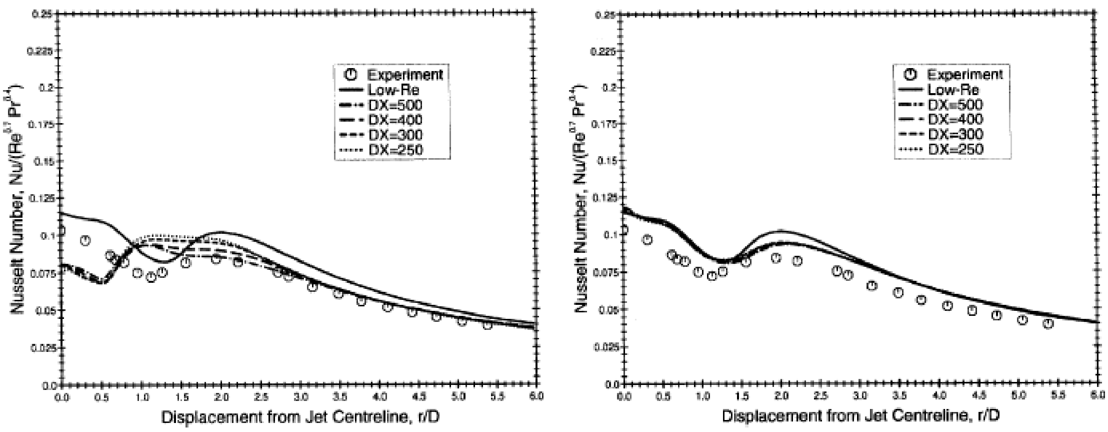

Figure 5. Nusselt number predictions for the impinging jet ($H/D = 4, \mathrm{Re} = 70,000$) using the nonlinear k–ε model; broken lines are wall-function results with different near-wall cell sizes; (left) Chieng and Launder wall function; (right) UMIST-N wall function.

	Wall functions		
	Chieng and Launder	UMIST-N	Low-Re, Craft et al.
Number of nodes	70×45	70×45 (+ 40)	70×90
CPU time per iteration (s)	0.158	0.260	0.324
No. of iterations	1,426	1,380	9,116
Total CPU time (s)	226	359	2,955
Relative CPU time	1	1.59	13.08

Free Rotating Disc Flow

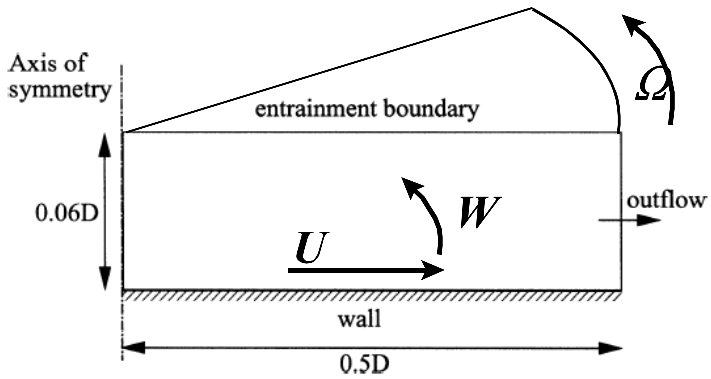

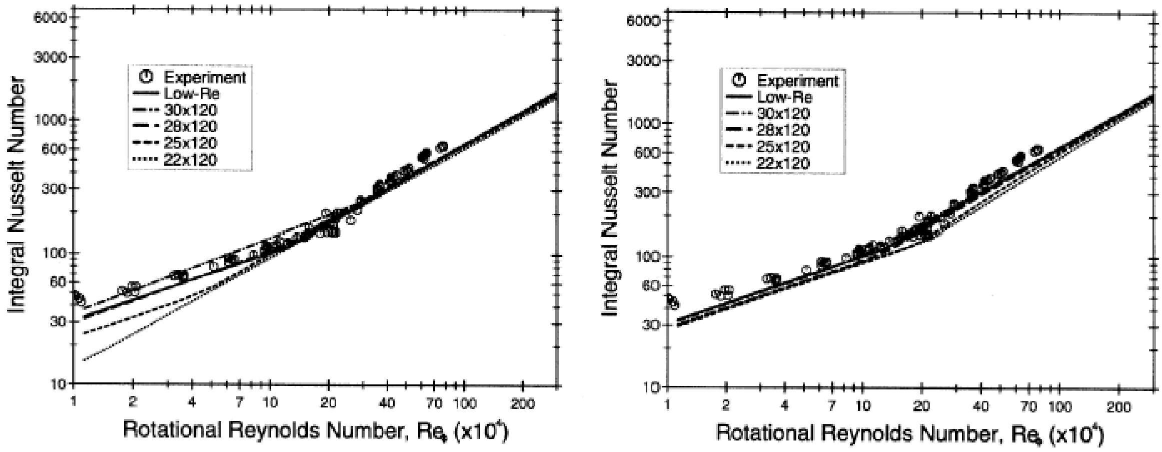

Figure 8. Predicted integral Nusselt number in the free-disc flow using the linear $k - \varepsilon$ model with: (left) Chieng and Launder wall function; (right) UMIST-*N* wall function. Solid line, low-Re model; broken lines, wall function results for different grid arrangements; ○, experimental values from Cobb and Saunders [24].

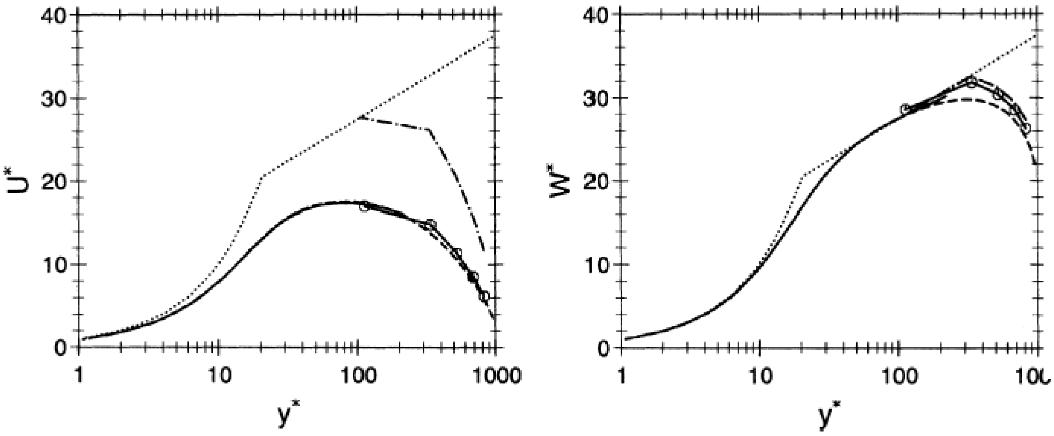

Figure 9. Velocity profiles for the free-disc flow at $\mathrm{Re}_\phi = 1.0 \times 10^6$ using wall-law axes; (left) radial *U*-velocity and (right) tangential *W*-velocity; –○–, UMIST-*N* wall function (circles indicate the position of primary grid nodes and the solid line without symbols represents the solution across the subgrid); – – –, low-Re model; –·–, Chieng and Launder wall function; ···, "universal" log-law.

3-D U-Bend Flow

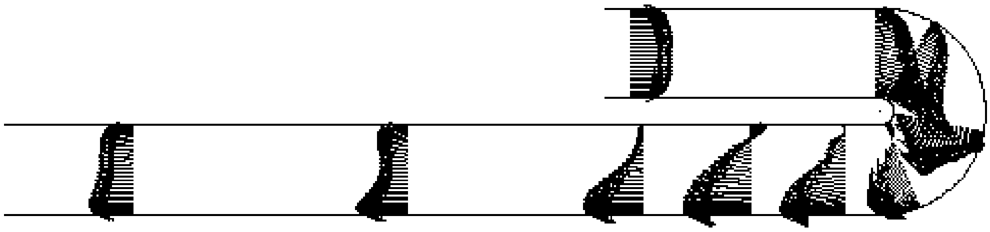

Streamwise Velocity Comparisons

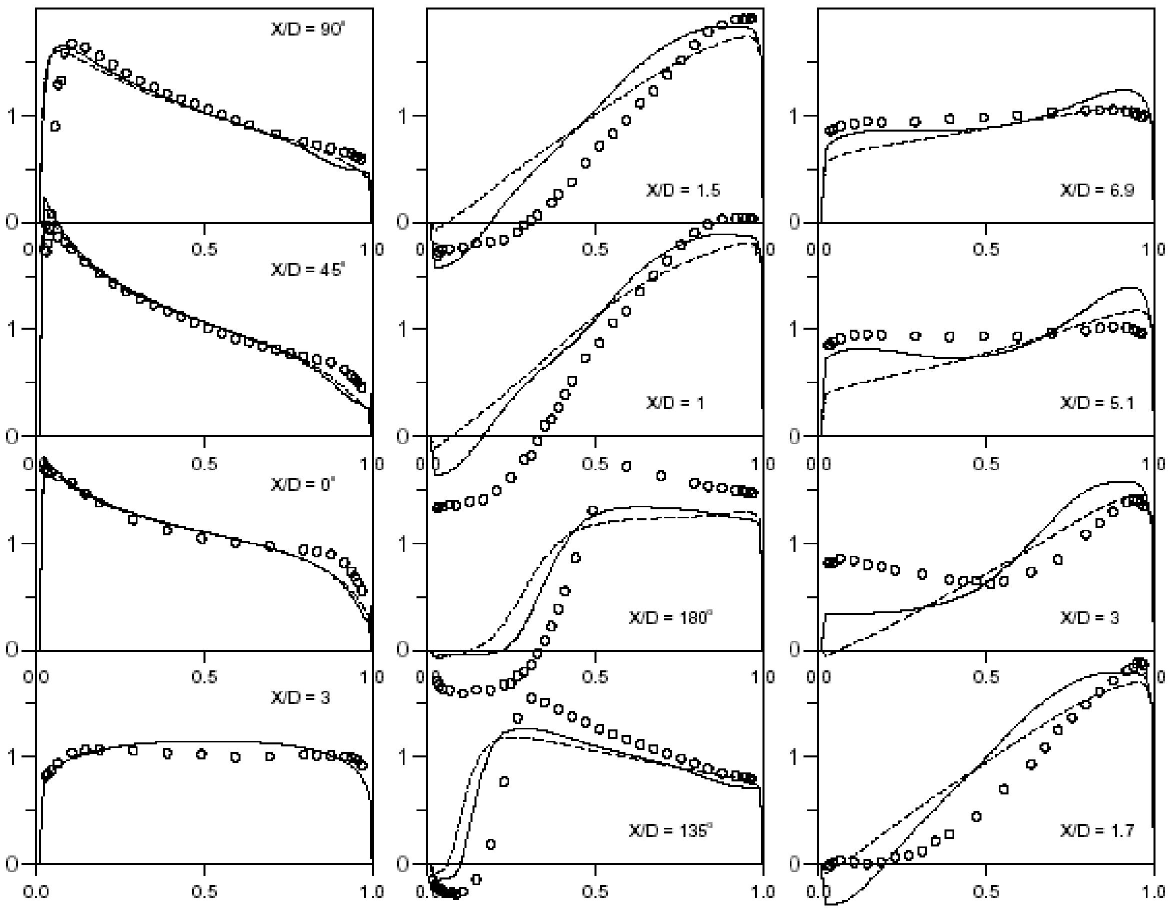

____ : DSM /UMIST-N   ------- k-ϵ/UMIST-N

3-D U-Bend Flow

Comparisons of Side-averaged Nusselt Number

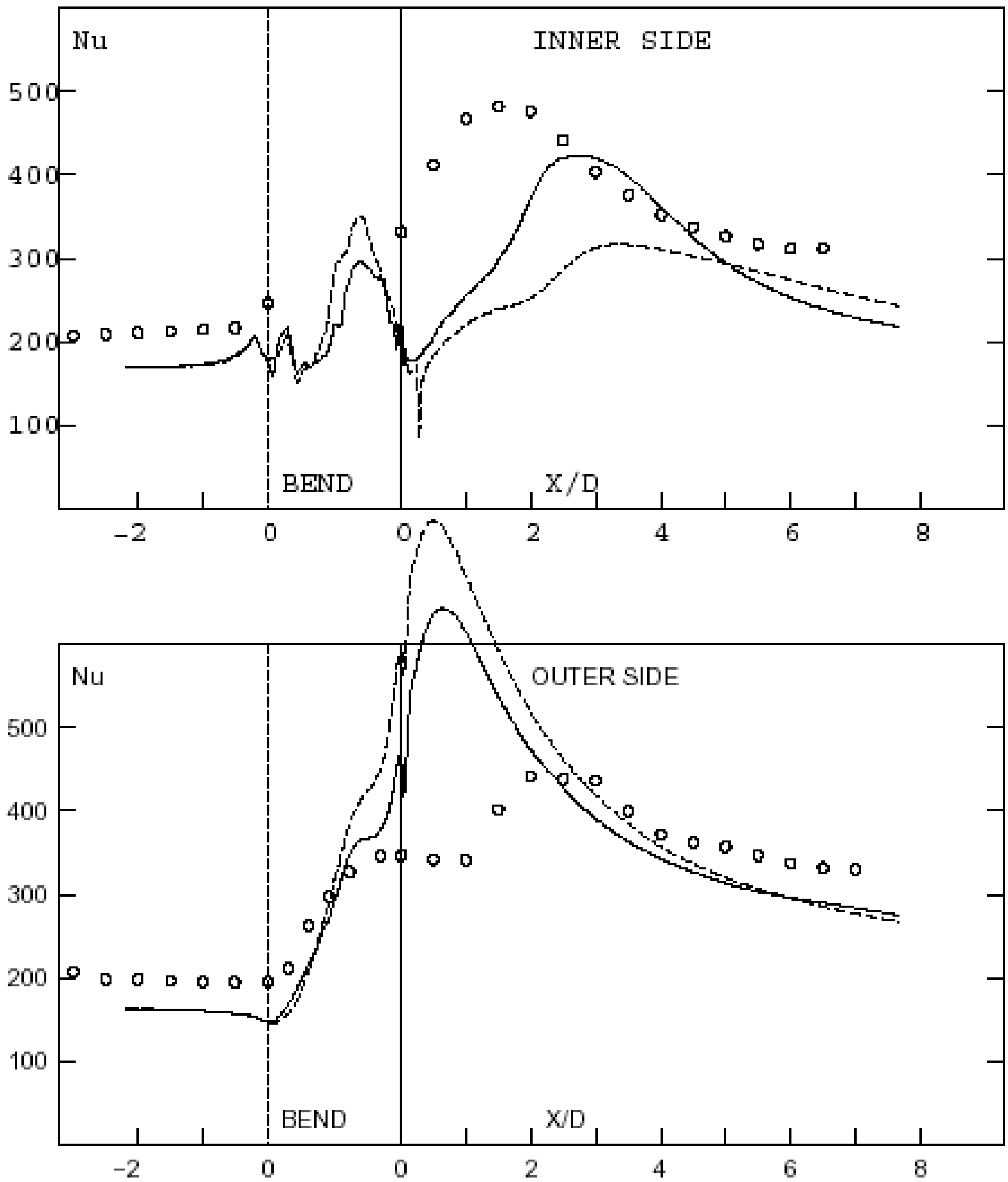

____ : DSM /UMIST-N ------- k-ϵ/UMIST-N

Other Applications of the Numerical Wall Function

- 3-D Flow over the Ahmed Body.
- Rotating Cavity Flows
- Abrupt Pipe Expansion

7 . Concluding Remarks

- Two wall-function strategies have been presented which:

  - Do not rely on either the log-law, or a prescribed total shear-stress variation.
  - Solve simplified momentum and enthalpy equations across the near-wall cells.

- The Analytical Wall Function, UMIST-A:

  - Is as computationally efficient as the conventional approach.
  - In many complex flows results in predictions of the same quality as a low-Reynolds-number approach.
  - Has been also extended to include the effects of small-scale surface roughness.

- The Numerical Wall Function, UMIST-N:

    - Increases computational overheads, relative to the conventional approach, by 60% to 100%.
    - Results in predictions similar to those of low-Re models at only a fraction of the cost.
- Both approaches have been implemented in 3-dimensional general-geometry codes.

- Application of both approaches to more cases is in progress.

Bibliography

1. Chieng C C and Launder B E.
On the calculation of turbulent heat transport downstream from an abrupt pipe expansion ,Numerical Heat Transfer, **vol 3**, pp 189-207, 1980.

2. Johnson R W and Launder B E .
Discussion of ' On the calculation of turbulent heat transport downstream from an abrupt pipe expansion, Numerical Heat Transfer, **vol 5**, pp 493-496, 1982.

3. Amano R
Development of Turbulence Near0Wall Model and its Application to Separated and Reattached Flows, Numerical Heat Transfer, Vol 7, pp 59-76, 1984.

4. Launder B. E.
On the computation o convective heat transfer in complex turbulent flows, ASME, Journal of Heat Transfer, **110**,pp1112-1128, Nov. 1988

5. M Ciofallo and W M Collins
k-ϵ predictions of heat transfer in turbulent re-circulating flows using an improved wall treatment, Numerical Heat Transfer, Vol 15, pp 21-47, 1989.

6. T. J. Craft, A Gerasimov, H. Iacovides and B.E. Launder
Progress in the generalisation of wall-function treatments, International Journal of Heat and Fluid Flow, **23**, 148-16,2002

7. T. J. Craft., S. E. Gant, H. Iacovides and B. E. Launder
A New Wall-Function strategy for Complex Turbulent Flows, Numerical Heat Transfer. Part B: Fundamentals, **45**, No 4, pp 301-318, 2004

8. T.J.Craft, S.E. Gant, A.V. Gerasimov, H. Iacovides and B.E. Launder.
Numerical Modelling of Heat Transfer in Wall-Adjacent Turbulent Flows, Chapter 11, Numerical Heat Transfer Handbook., 2004.

9. T.J. Craft, A. V. Gerasimov, H. Iacovides, J. W. Kidger and B. E. Launder
The Negatively Buoyant Turbulent Wall Jet:Performance of alternative options in RANS Modelling., To Appear, International Journal of Heat and Fluid Flow, 2004.